



## A Comparative Study of Particle Size Measurement of Silver, Gold and Silica Sand Nanoparticles with Different Nanometrological Techniques



CrossMark

Rania Sayed <sup>1\*</sup>, Moustafa M. Elmasri <sup>2</sup>, Abdelghaffar S. Dhmees <sup>3</sup>

<sup>1</sup>. Material Testing and Chemical Surface Analysis Laboratory, National Institute of Standards, P. O. Box: 136 Giza, Code No. 12211, Giza, Egypt

<sup>2</sup>. Inorganic and Electrochemistry Laboratory, National Institute of Standards, P. O. Box: 136 Giza, Code No. 12211, Giza, Egypt

<sup>3</sup>. Analysis and Evaluation Department, Egyptian Petroleum Research Institute, Cairo 11727, Egypt

### Abstract

The composition, size, shape, charge, and surface chemistry of nanoparticles are critical properties that need to be tightly controlled and measured for a wide range of applications, from the production of nanoparticle reference materials to the development of new materials products with nanometer-sized dimensions. Measuring the particle size of nanomaterials help to evaluate their safety, quality and efficiency. In fact, there is not a single characterization technique to measure the particle size of nanoparticles accurately. This comparative study introduced three nano-metrological techniques: X-ray diffraction (XRD), dynamic light scattering (DLS), and a high-resolution transmission electron microscope (HR-TEM), to measure particle size and explain the difference in sizing measurements that were performed. Five samples of nanoparticles were analyzed; commercial Silver nanoparticles (Two samples), biosynthesized Silver nanoparticles, biosynthesized Gold nanoparticles and ballistc milled Silica sand nanoparticles. The particle size measured with the non-destructive DLS technique was close to the crystallite size was calculated from the XRD pattern by using Debye-Scherrer's equation. The particle size as measured by the high-resolution sizing technique (TEM) was the most accurate measurement because the microscope directly observed and measured individual nanoparticles. A scanning electron microscope (SEM) was used to investigate the morphology of the five analyzed samples. The uncertainty in particle size measurements was estimated from statistical analysis of repeated readings of the measured value.

**Keywords:** Particle size measurements; Nanometrology, Debye-Scherrer's equation, SEM, HR-TEM, DLS, Estimated uncertainty

### 1- Introduction

In the world of nanotechnology, the nanoparticles size and shape has attracted the attention of researchers toward their potential applications such as antimicrobial textile [1-3] and finishing treatments [4,5], fabrication of reference materials [6,7], water disinfectant [8-12], diagnosis of diseases [13-16], Biosensing [17-19], solar cell [20-23], energy storage [24-27], environmental remediation [28-31], additives [32-35], and many others widespread application.

The science of measurement at the nanoscale level is known as nanometrology. Nanometrology has a key role in developing nanometer-sized dimensions products [36]. Fundamental studies and new technological applications need nanoparticles with uniform shapes and sizes [37]. Nanometrology techniques and standards are required to control fabrication, production and characterization of

nanomaterials [38-40]. Due to the extremely small size of nanomaterials (less than 100 nm) and low quantity in laboratory-scale production, more precise techniques and international standards are required for their characterization [41-43]. International guidelines and specification standards relating to classification, measurements and characterization of nanomaterials have been published by the international organization for standardization (ISO) such as ISO/TS 12805:2011 (Materials specifications — Guidance on specifying nano-objects), ISO 17200:2020 (Nanoparticles in powder form Characteristics and measurements), ISO 21363:2020 (Measurements of particle size and shape distributions by transmission electron microscopy), and ISO 19749:2021 (Measurements of particle size and shape distributions by scanning electron microscopy).

Correspondence: rsayed.nis@gmail.com

**Receive Date:** 21 July 2022, **Revise Date:** 05 August 2022, **Accept Date:** 07 August 2022, **First Publish Date:** 07 August 2022

DOI: 10.21608/EJCHEM.2022.150764.6562

©2023 National Information and Documentation Center (NIDOC)

Nanometrological measurements can be varied from the length, size, shape, aspect ratio and size distribution to force, mass, chemical composition, nanoparticle concentration, and other properties [36,44]. Measurements at the nanoscale level need high precision and effective methods of measurement [45,46]. The great challenge of nanometrology is reaching metrological traceability and estimating uncertainty in measurement at the nanoscale [38]. Accurate measurements of nanoparticles affect significantly their commercial applications. Nanometrological techniques such as high-resolution transmission electron microscope (HR-TEM), scanning electron microscope (SEM), dynamic light scattering (DLS), and x-ray diffraction (XRD) are required to define the size, shape, particle size distribution (PSD), and crystal structure of the nanomaterials precisely [47-50]. The two most famous methods used for size measurements of nanoparticles are the light scattering method, which uses dynamic fluctuation of the scattered light to calculate the average particle size, and the microscopic techniques which measures particle size from particle images [51].

To achieve good quality measurements and understand the results, the uncertainty of measurements has to be calculated. Uncertainty is known as a quantification of the doubt about the measurement result while error is the difference between the 'measured value' and the 'true value' of the thing being measured [52,53]. Uncertainty type A,  $U_A$ , is usually estimated from statistical analysis of repeated readings of measured value  $U_A = S/\sqrt{n}$ , where S is the standard deviation and n is the number of measurements. Uncertainty type B,  $U_B$ , estimates from calibration certificates of devices and any other information. Both types of uncertainty are needed in most measurement situations. In this experiment, the size, shape, particle size distribution (PSD) measurements, and crystal structure of the nanomaterials were studied by using different nanometrological techniques. Different samples of Silver nanoparticles, Gold nanoparticles and Silica sand nanoparticles were investigated.

## 2- Materials and Experimental Methods

In this study, five samples of nanomaterials were analyzed. High pure powder of Ag NPs was purchased from Sigma Aldrich (Ag NPs, Sigma), well dispersed solution of Ag NPs was ordered from Metalon (Ag NPs, Metalon), biosynthesized Silver nanoparticles (Ag NPs) from actinomycete strain; *Streptomyces* sp. U13 (KP109813), isolated from sandstone rock, biosynthesized Gold nanoparticles (Au NPs) from actinomycete strain; *Streptomyces* sp. U30 (KP109810), isolated from metal containing rock [57], and physically synthesized Silica sand nanoparticles (SS NPs) by using ball milling [58], were

characterized by using different nanometrological techniques.

### Characterization

UV-Vis spectrophotometer (Shimadzu, UV3101PC, Japan) was used to confirm the formation of biosynthesized nanoparticles in solution at room temperature. XRD analysis of the prepared samples of nanoparticles was done using a Pananalytical X'pert Pro diffractometer with Cu K $\alpha$ 1 radiation ( $\lambda=1.540595$  Å) (Malvern, GH Eindhoven, The Netherlands). Particle size analysis of the five analyzed samples of nanoparticles was carried out precisely with dynamic light scattering (DLS) (Nano ZS90, Malvern Instrument). A He-Ne laser, 633 nm, was used as a light source. Particle size was measured using the method of dynamic light scattering where the scattered light was collected by using an avalanche photodiode detector (APD). The size and shape of nanoparticles were investigated by utilizing a high-resolution transmission electron microscope (HR-TEM, Jeol JEM 2100) with an acceleration voltage of 200 kV. The surface morphology of nanoparticles for all samples was examined by A CARL ZEISS SIGMA 500vp scanning electron microscopy (SEM) (Zeiss, Berlin, Germany).

### Synthesis of Au NPs, Ag NPs and SS NPs

Au NPs and Ag NPs were synthesized biologically from actinomycete strain; *Streptomyces* sp. U30 (KP109810), isolated from metal containing rock [57] and actinomycete strain; *Streptomyces* sp. U13 (KP109813), isolated from sandstone rock, respectively. UV-Vis spectrophotometer results indicated that the biosynthesis of Gold nanoparticles was confirmed by a well-defined absorption peak that appeared at 524 nm [57]. The bio-formation of Ag NPs was confirmed by an absorption beak recorded at 434 nm. SS NPs were physically synthesized by using the ball mill technique. Ball mill was utilized to process sand nature particles, collected from the beach area of Rosetta in Egypt to the nanoparticles [58]. TEM images revealed that the diameter size of Au NPs, Ag NPs and SS NPs were ranging from 11.96 to 34.62, 3.91 to 37.83, and 9.87 to 117.02 nm, respectively. Ball milled Silica sand displayed that the SS NPs are not uniform with a high agglomeration among the particles because the mechanical parts of ball milling device, used to shape nanoparticles, are stiff and hard.

## 3- Results and Discussion

### Particle size measurement of nanomaterials X-ray diffraction studies

X-ray diffraction technique is considered as a primary characterization tool in nanoparticle research for achieving critical features such as crystal structure and crystallite size. In nanocrystalline materials, the randomly oriented crystals cause broadening of

diffraction peaks due to the absence of total constructive and destructive interferences of X-rays in a finite sized lattice. The Debye-Scherrer's formula,  $d = K\lambda/\beta\cos\theta$ , is the most widely used method for estimating the crystallite size from the full width at half maximum (FWHM) of a diffraction peak broadening [59-61]. Where  $d$  is the crystallite size in nm,  $\lambda$  is the X-ray wavelength ( $Cu_{K\alpha}$  wavelength,  $\lambda=1.540595$  Å),  $\beta$  is the full width at half maximum (FWHM) of the peak in radian,  $\theta$  is the X-rays incident angle in degree and  $K$  is the Scherrer constant that is close to unity.

To avoid error in the X-ray diffraction pattern of the analyzed samples, the performance of the X-ray diffractometer, in terms of peak positions and resolution, was checked using the standard silicon single crystal specimen at the experiment conditions. The XRD pattern of the five analyzed samples were collected at room temperature (Fig. 1) and the crystallite size parameter was estimated from XRD peaks by using the Scherrer equation as displayed in (Table 1). XRD of Ag NPs (Metalon) showed a hump at  $2\theta$  of  $27.008^\circ$ , which indicates that Ag NPs (Metalon) is amorphous as in (Fig. 1a). XRD pattern of powder of Ag NPs (Sigma Aldrich) presented four distinct diffraction peaks at  $2\theta$  of  $38.11^\circ$ ,  $44.32^\circ$ ,  $64.50^\circ$  and  $77.45^\circ$  as displayed in (Fig. 1b), these peaks could be attributed to the (111), (200), (220) and (311) crystallographic planes of the face centred cubic Ag crystal. XRD of Ag NPs (Biosynthesized) was illustrated in (Fig. 1c), the XRD pattern showed the Bragg's diffraction peaks at  $38.16^\circ$  and  $45.04^\circ$  which corresponds to the (111) and (200) diffraction plane of Silver and the other peaks at  $31.55^\circ$  and  $32.78^\circ$  may be appeared because of the crystallization of the bio-organic phase [62,63]. XRD pattern of the Au NPs displayed in (Fig. 1d), the fcc crystal structure of Gold is confirmed by the Bragg reflections (111), (200), (220), (311) and (222) at  $2\theta$  of  $35.95^\circ$ ,  $41.85^\circ$ ,  $61.51^\circ$ ,  $75.26^\circ$  and  $82.21^\circ$  respectively. The crystallite size is calculated based on the four peaks (111), (200), (220) and (311) as shown in (Table 1). XRD analysis of powder of Silica sand nanoparticles (SS NPs) was shown in (Fig. 1e). XRD pattern demonstrated peaks at  $20.76^\circ$ ,  $26.57^\circ$ ,  $35.52^\circ$  and  $45.82^\circ$  corresponded to the (100), (101), (110) and (201) and the unknown peak at  $30.45^\circ$ . The obtained results of XRD analysis were consistent with the previously published reports of Silver nanoparticles [64-68], Gold nanoparticles and Silica sand nanoparticles [69-71].

#### **DLS method**

For achieving accurate measurements of particle size by using DLS method, ISO recommendation has to be followed. ISO 22412:2017 (Particle size analysis

— Dynamic light scattering (DLS)) was published to provide an estimation of the average particle size and particle size distribution (PSD) of nanoparticles. Dynamic light scattering (DLS) is a standard technique utilized to measure the size distribution of nanoparticles in suspension. DLS method probes the hydrodynamic mobility of the particles dispersed in liquids [51] and determines the size of the particles from fluctuations of the scattered light resulting from the Brownian motion of the particles. The analysis assumes that each particle is a perfect sphere and the measured average size of nanoparticles is the equivalent spherical size. When aggregation of nanoparticles exists in nanoparticle suspension, the measured value of particle size will be significantly biased and the aggregation treated as a single particle. In this study, the liquid suspensions of nanoparticles were treated for 5 mins in an ultrasonic bath to achieve a well-dispersed suspension. The Z average values of the five analyzed samples of nanoparticles were reported as the mean diameter of nanoparticles in (Table 2). Particle size distribution (PDS) measurements of the five analyzed samples, that were measured by the DLS method, were displayed in (Fig. 2). Three measurements for each sample were presented. Uncertainty in particle size measurements,  $U$ , was estimated and represented in (Table 3).

#### **HR-TEM analyses and SEM imaging**

The international committee of nanotechnology (TC229) at the international organization for standardization (ISO) has published recent standards dealing with the morphology of nanoparticles, such as ISO 21363:2020 (Nanotechnologies – Measurements of particle size and shape distributions by transmission electron microscope) and ISO 19749:2021 (Nanotechnologies — Measurements of particle size and shape distributions by scanning electron microscopy). For particle size measurement, the microscope is the only accurate method that directly observes and measures individual nanoparticles [72]. To investigate the size and shape of nanoparticles, TEM analyses and SEM morphological studies were carried out for the five samples of nanomaterials. TEM analyses were performed by using the high-resolution transmission electron microscope (HR-TEM) operated at 200 keV, the samples were prepared by putting a drop of each solution on a carbon/copper grid. Shape investigation of nanoparticles was done by using a scanning electron microscope (SEM), the samples were prepared on a graphite bulk substrate. For TEM analyses, different sections of the samples were studied to reveal the diameter of nanoparticles.

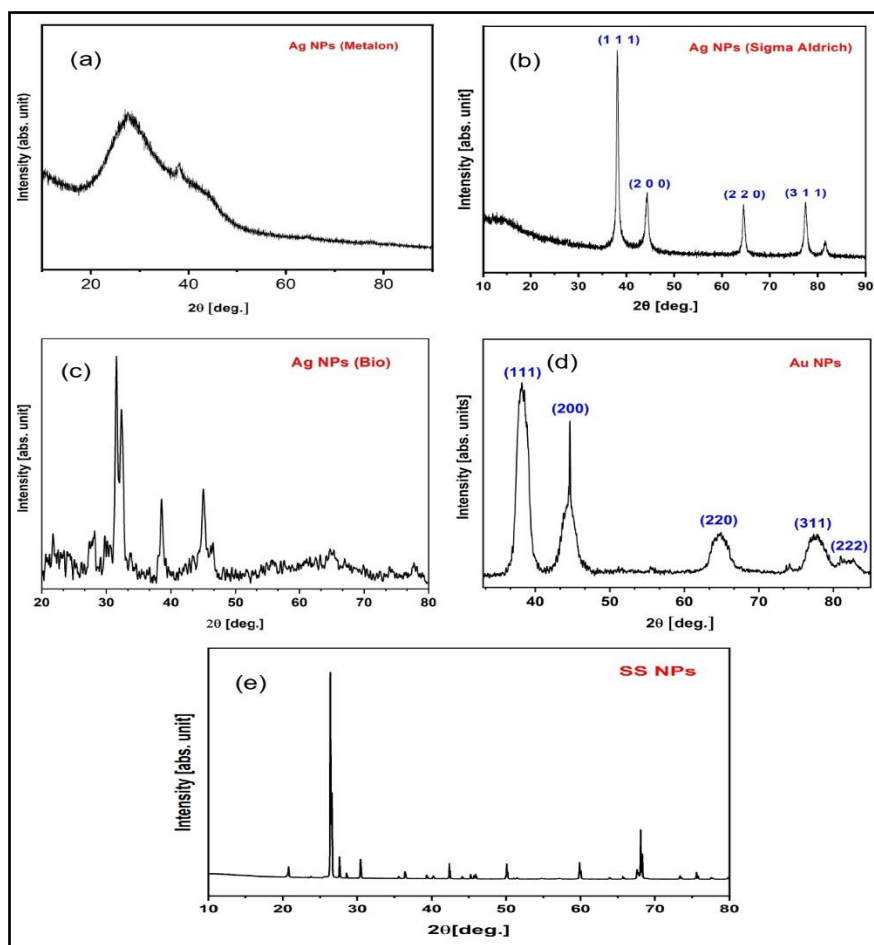


**Figure 1.** X-ray diffraction analysis of the different nanomaterials: (a) XRD of Ag NPs (Metalon), (b) XRD of Ag NPs (Sigma Aldrich), (c) XRD of Ag NPs (Biosynthesized), (d) XRD of Au NPs and (e) XRD of Silica sand NPs.

Table 1: The crystallite size parameter estimated from the XRD pattern (at each peak) by using the Scherrer equation for the analyzed samples of nanomaterials

	XRD analysis				
	Peak position [2 $\theta^\circ$ , degree]	hkl	FWHM [ $\beta$ , Radians]	Crystallite size [d, nm]	Average [d, nm]
Ag NPs (Sigma Aldrich)	38.14	111	0.009539	160.76	<b>133.50</b>
	44.28	200	0.015495	100.98	
	64.52	220	0.01242	137.98	
	77.47	311	0.013836	134.28	
Ag NPs (Biosynthesized)	31.55	----	0.008225	183.11	<b>195.57</b>
	32.34	----	0.010517	143.48	
	38.54	111	0.005269	291.37	
	45.01	200	0.009547	164.32	
Au NPs (Biosynthesized)	35.95	111	0.030644	49.72	<b>101.66</b>
	41.85	200	0.005632	275.52	
	61.51	220	0.04341	38.85	
	75.26	311	0.042995	42.56	
SS NPs (Physical synthesised)	20.76	100	0.001871	787.34	<b>1027.86</b>
	26.57	101	0.001758	847.02	
	30.45	----	0.00224	670.65	
	35.52	110	0.000924	1647.01	
Ag NPs (Metalon)	45.82	201	0.001325	1187.26	
			Amorphous		

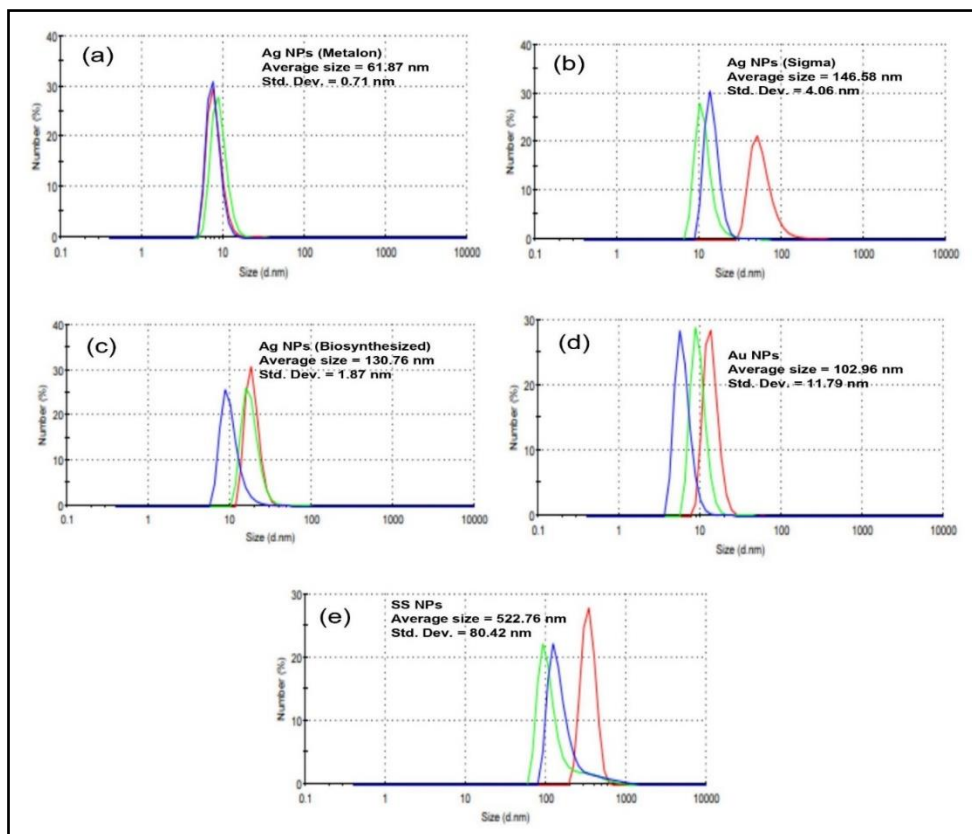


**Figure 2.** Particle size distribution (PSD) of nanoparticles obtained by DLS. (a) Silver nanoparticles (Metalon), (b) Silver nanoparticles (Sigma), (c) Silver nanoparticles (Biosynthesized), (d) Gold nanoparticles and (e) Silica sand nanoparticles. Red, green and blue curves are three repeated measurements for each sample.

The mean diameter and standard deviation were about  $16.52 \pm 7.79$ ,  $18.94 \pm 7.8$ ,  $15.3 \pm 9.1$ ,  $23.94 \pm 6.4$ , and  $45.2 \pm 34.28$  nm for Ag NPs (Metalon), Ag NPs (Sigma), Ag NPs (Biosynthesized), Au NPs, and SS NPs respectively. Uncertainty in particle size measurements, UA, was estimated and represented in table (3). TEM images of the five analysed samples indicated that Ag NPs (Metalon) were spherical and well dispersed (Fig. 3a), Ag NPs (Sigma) were spherical and highly aggregated (Fig. 3d), Ag NPs (Biosynthesized) were spherical and hexagonal in

shape and there was a little aggregation as shown in (Fig. 3g), Au NPs were hexagonal and triangular in shape and there was a little aggregation (Fig. 3j) and SS NPs were random and highly aggregated (Fig. 3m). These results were confirmed by the results obtained from SEM images (Fig. 3b, 3e, 3h, 3k and 3n). The histogram of the particle size distribution (PSD) extracted from statistical analysis of HR-TEM images were shown in (Fig. 3c, 3f, 3i, 3l and 3o), it reveals the range of the particle size.

Table 2 Particle size measurements of the five analyzed samples with different nanometrological techniques

Method	Physical principle	Mean size of nanoparticles				SS NPs
		Ag NPs (Metalon)	Ag NPs (Sigma)	Ag NPs (Bio)	Au NPs (Bio)	
XRD	X-ray diffraction	N/A	133.50	195.57	101.66	1027.86
DLS	Light scattering	61.87	146.58	130.76	102.96	522.76
HR-TEM	Imaging/particle counting	16.52	18.49	15.3	23.49	45.2
SEM	Imaging/particle shape	Spherical & hexagonal	Spherical	Spherical & hexagonal	Triangular & hexagonal	Random

Table 3: Particle size measurements of the five analyzed samples combined with estimated uncertainty (U) at level of confidence 95%.

Mean particle size of nanoparticles with uncertainty type A & B				
	Mean size from TEM	U	Mean size from DLS	U
Ag NPs (Metalon)	16.52	2.206	61.87	1
Ag NPs (Sigma Aldrich)	18.94	2.209	146.58	4.726
Ag NPs (Biosynthesized)	15.3	3.325	130.76	1.1179
Au (Biosynthesized)	23.94	1.814	102.96	13.626
SS NPs (Ball milled)	45.20	8.852	522.76	92.866

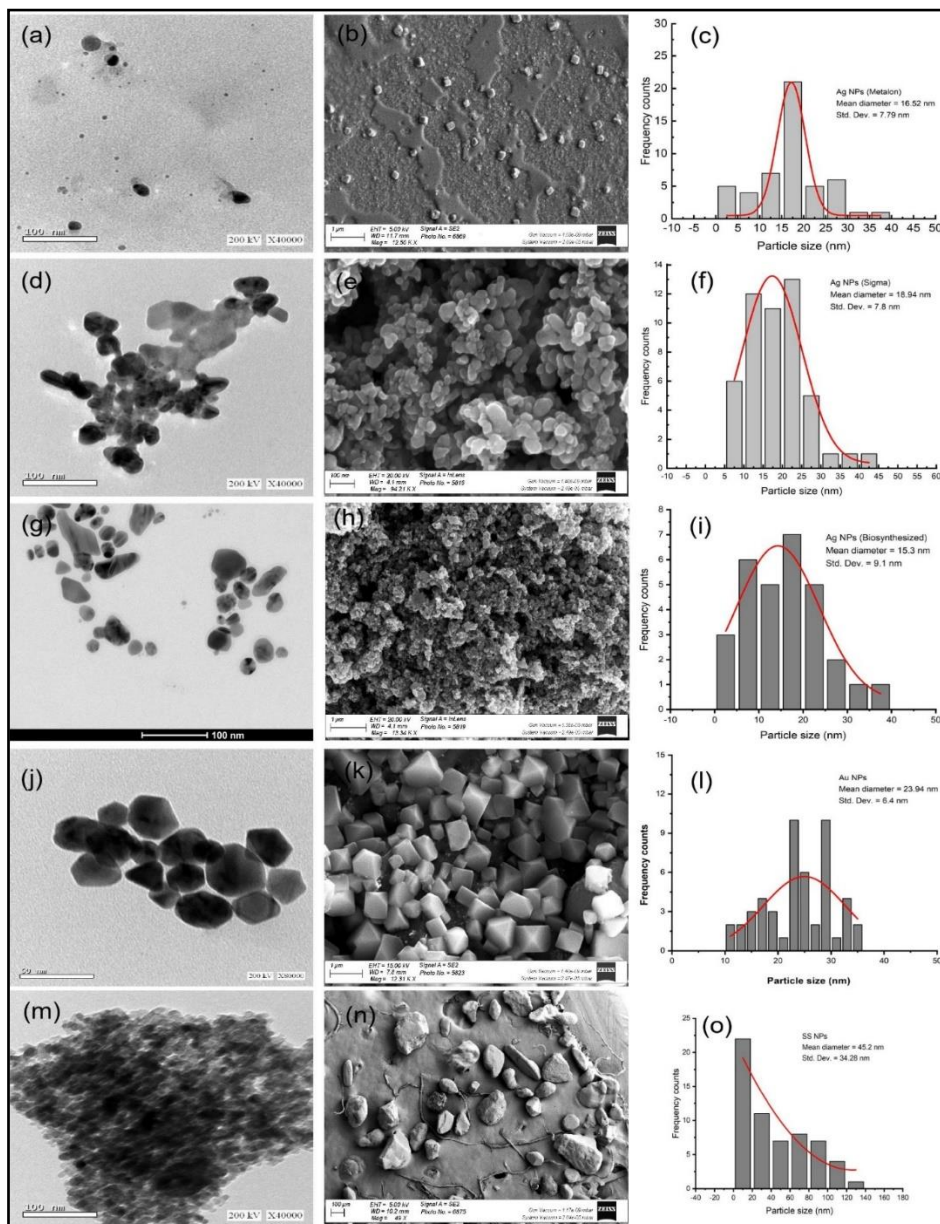


Figure 3: TEM and SEM analysis of nanoparticles. (a) HR-TEM image of Ag NPs (Metalon), (b) SEM image of Ag NPs (Metalon), (c) Histogram of the particle size distribution of Ag NPs (Metalon), (d) HR-TEM Image of Ag NPs (Sigma), (e) SEM image of Ag NPs (Sigma), (f) Histogram of the particle size distribution of Ag NPs (Sigma), (g) HR-TEM Image of Ag NPs (Biosynthesized), (h) SEM image of Ag NPs (Biosynthesized), (i) Histogram of the particle size distribution of Ag NPs (Biosynthesized), (j) HR-TEM Image of Au NPs (Biosynthesized), (k) SEM image of Au NPs (Biosynthesized), (l) Histogram of the particle size distribution of Au NPs (Biosynthesized), (m) HR-TEM Image of SS NPs, (n) SEM image of SS NPs and (o) Histogram of the particle size distribution of SS NPs. The histograms of the particle size distribution of the five analyzed samples are based on TEM image analysis and the red line is a Gaussian distribution fit.

The values of mean size of nanoparticles, obtained by X-ray diffraction and dynamic light scattering, were consistent for Ag NPs (Sigma), Ag NPs (Biosynthesized) and Au NPs (Biosynthesized) while there was a big difference between the two values of ball milled SS NPs due to the high agglomeration and random shape of the particles. The most accurate results of the mean particle size were achieved by the HR-TEM. TEM results based on direct measurement of the size of individual nanoparticles. In literature [71-73], the value of particle size obtained from XRD calculations should be the same as the value extracted from TEM images. Actually, this could be happened at a single peak broadening of XRD pattern. In this study, the particle size calculated at each peak of XRD peaks then the mean value was considered as the particle size. Also, HR-TEM measurement done for 50 nanoparticles only while the XRD and DLS measurement carried out for the whole sample of nanoparticles.

### 1. Conclusions

To conclude, there is not a single measuring technique to determine and provide all the information on particle size measurement. In this comparative study, different nanometrological techniques, XRD, DLS, HR-TEM, and SEM, were used to measure the particle size and provide the morphology of silver, Gold and Silica sand nanoparticles. XRD is a non-destructive tool for calculating the crystallite size of nanoparticles from the XRD pattern by using Debye-Scherrer's formula. DLS is a fast and affordable tool to determine the mean size and size distribution of nanoparticles but can't differentiate the small aggregation of nanoparticles from large particles. On the contrary, HR-TEM allows direct observation of the size and shape of individual nanoparticles on a substrate even with the presence of large aggregates leading to accurate measurements of particle size. In this experiment, the obtained results of calculated crystallite size of nanoparticles from XRD were close to the average size of nanoparticles measured by DLS. The mean diameter of nanoparticles that measured by HR-TEM has the lowest value of the particle size measurement. It is based on the image analysis of 50 particles. Statistical analysis of TEM results produced the particle size distribution (PSD). The scanning electron microscope (SEM) is a highly precise imaging tool but it is not accurate for measuring the size of the nanoparticle.

### 2. Conflicts of interest

There are no conflicts to declare.

### 3. References

- [1] Hasan R et al. Production of antimicrobial textiles by using copper oxide nanoparticles. *International Journal of Contemporary Research and Review* **9**, 20195-20202 (2018). <https://doi.org/10.15520/ijcrr/2018/9/08/564>
- [2] Zille A et al. Gold nanoparticles synthesis and antimicrobial effect on fibrous materials. *Nanomaterials* **11**, 1-37(2021). <https://doi.org/10.3390/nano11051067>
- [3] Ballottin D et al. Antimicrobial textiles: Biogenic Silvernanoparticles against *Candida* and *Xanthomonas*. *Materials Science and Engineering C* **75**,582–589(2017). <https://doi.org/10.1016/j.msec.2017.02.110>
- [4] Sukanta P et al. Applications of nanotechnology for antibacterial finishing textiles: A Review. *Sensor Letters* **18**, 1-12(2020). <https://doi.org/10.1166/sl.2020.4260>
- [5] Yunping W et al. Fabrication of cotton fabrics with durable antibacterial activities finishing by Ag nanoparticles. *Textile Research Journal* **89**, 867-880(2018). <https://doi.org/10.1177/0040517518758002>
- [6] Kestens V et al. A new certified reference material for size and shape analysis of nanorods using electron microscopy. *Analytical and Bioanalytical Chemistry* **413**, 141–157(2020). <https://doi.org/10.1007/s00216-020-02984-z>
- [7] Linsinger et al. Reference materials for measuring the size of nanoparticles. *Trends in Analytical Chemistry* **30**,18-27(2011). <https://doi.org/10.1016/j.trac.2010.09.005>
- [8] Dimapilis E. A. S. et al. Zinc oxide nanoparticles for water disinfection. *Sustainable Environment Research* **28**, 47-56(2018). <https://doi.org/10.1016/j.serj.2017.10.001>
- [9] Al-Issai L et al. Use of nanoparticles for the disinfection of desalinated water. *Water* **11**, 1-20(2019). <https://doi.org/10.3390/w11030559>
- [10] Robbie V A and Onita D. Basu Silverand zinc oxide nanoparticle disinfection in water treatment applications: synergy and water quality influences. *H<sub>2</sub>Open Journal* **4**, 114-128(2021). <https://doi.org/10.2166/h2oj.2021.098>
- [11] Haijiao Lu et al. An overview of nanomaterials for water and wastewater treatment. *Advances in Materials Science and Engineering* **2016**, 1-10(2016). <https://doi.org/10.1155/2016/4964828>
- [12] Simeonidis K et al. Implementing nanoparticles for competitive drinking water purification. *Environmental Chemistry Letters* **17**, 705–719(2018). <https://doi.org/10.1007/s10311-018-00821-5>
- [13] Azzawi M, Seifalian A and Ahmed W Nanotechnology for the diagnosis and treatment of diseases. *Nanomedicine* **11**, 2025-2027(2016). <https://doi.org/10.2217/nnm-2016-8000>
- [14] Yaqoob S B et al. Gold, silver, and palladium nanoparticles: A chemical tool for biomedical applications. *Front. Chem.* **8**, 1-15(2020). <https://doi.org/10.3389/fchem.2020.00376>
- [15] Muneeer M et al. Diagnosis and treatment of diseases by using metallic nanoparticles-A review. *International Journal of Global Science* **3**, 27-35(2020). <http://www.rndjournals.com>
- [16] Paluszkiwicz P et al. The application of nanoparticles in diagnosis and treatment of kidney diseases. *Int. J. Mol. Sci.* **23**, 1-28(2021). <https://doi.org/10.3390/ijms23010131>
- [17] Malekzad H et al. Noble metal nanoparticles in biosensors: recent studies and applications. *Nanotechnol Rev.* **6**, 301–329(2017). <https://doi.org/10.1515/ntrev-2016-0014>
- [18] Peltomaa R et al. Biosensing based on upconversion nanoparticles for food quality and safety applications. *Analyst* **146**, 13–32(2021).

- <https://doi.org/10.1039/d0an01883j>
- [19] [Kairdolf](#) A B, Qian X and Nie S Bioconjugated nanoparticles for biosensing, in vivo imaging, and medical diagnostics. *Anal. Chem.* **89**,1015–1031(2017).  
<https://doi.org/10.1021/acs.analchem.6b04873>
- [20] Wibowo A et al. ZnO nanostructured materials for emerging solar cell applications. *RSC Adv.* **10**, 42838–42859(2020). <https://doi.org/10.1039/d0ra07689a>
- [21] Wei W et al. Advanced nanomaterials and nanotechnologies for solar energy. *International Journal of Photoenergy* **2019**, 1-2(2019).  
<https://doi.org/10.1155/2019/8437964>
- [22] Rai P. Plasmonic noble metal and metal oxide core-shell nanoparticles for dye-sensitized solar cell applications. *Sustainable Energy Fuels* **3**, 63–91(2019). <https://doi.org/10.1039/C8SE00036J>
- [23] [Panahi-Kalamuei](#) M et al. Facile microwave synthesis, characterization, and solar cell application of selenium nanoparticles. *Journal of Alloys and Compounds* **617**, 627–632(2014).  
<https://doi.org/10.1016/j.jallcom.2014.07.174>
- [24] Xiaofeng S et al. Preparation of BaTiO<sub>3</sub>/low melting glass core-shell nanoparticles for energy storage capacitor applications. *J. Mater. Chem. A* **2**, 18087–18096(2014). <https://doi.org/10.1039/C4TA04282D>
- [25] X Song et al. (2018) General dimension-controlled synthesis of hollow carbon embedded with metal single atoms or core-shell nanoparticles for energy storage applications. *Adv. Energy Mater.* **8**, 1–13. <https://doi.org/10.1002/aenm.201801101>
- [26] Sheikholeslami M and Mahian O. Enhancement of PCM solidification using inorganic nanoparticles and an external magnetic field with application in energy storage systems. *Journal of Cleaner Production* **215**, 963–977(2019).  
<https://doi.org/10.1016/j.jclepro.2019.01.122>
- [27] Ying L et al. Structure control and performance improvement of carbon nanofibers containing a dispersion of silicon nanoparticles for energy storage. *CARBON* **51**, 185 – 194(2013).  
<https://doi.org/10.1016/j.carbon.2012.08.027>
- [28] Zhang Di et al. Carbon-stabilized [iron nanoparticles](#) for environmental remediation. *Nanoscale* **2**, 917–919(2010). <https://doi.org/10.1039/C0NR00065E>
- [29] Singh J et al. ‘Green’ synthesis of metals and their oxide nanoparticles: applications for environmental remediation. *Journal of Nanobiotechnology* **16**, 1–24(2018). <https://doi.org/10.1186/s12951-018-0408-4>
- [30] [Jiang](#) B et al. Advances of magnetic nanoparticles in environmental application: environmental remediation and (bio)sensors as case studies. *Environmental Science and Pollution Research* **25**, 30863–30879(2018).  
<https://doi.org/10.1007/s11356-018-3095-7>
- [31] Javed R et al. Role of capping agents in the application of nanoparticles in biomedicine and environmental remediation: recent trends and future prospects. *J Nanobiotechnol* **18**, 1–15(2020).  
<https://doi.org/10.1186/s12951-020-00704-4>
- [32] [Prabu](#) A Engine Characteristic Studies by Application of antioxidants and nanoparticles as additives in biodiesel diesel blends. *J. Energy Resour. Technol.* **140**, 1–7(2018). <https://doi.org/10.1115/1.4039736>
- [33] [Zhao](#) J et al. Nanolubricant additives: A review. *Friction* **9**, 891–917(2020).  
<https://doi.org/10.1007/s40544-020-0450-8>
- [34] [Contreras](#) O et al. Application of in-house prepared nanoparticles as filtration control additive to reduce formation damage. Paper presented at the SPE International Symposium and Exhibition on Formation Damage Control, Lafayette, Louisiana, USA, February 2014. <https://doi.org/10.2118/168116-MS>
- [35] Kumara C et al. Organic-modified Silvernanoparticles as lubricant additives. *ACS Appl. Mater. Interfaces* **9**, 37227–37237(2017).  
<https://doi.org/10.1021/acsami.7b13683>
- [36] Herrera-Basurto R and Simonet B M. Nanometrology. *Encyclopedia of Analytical Chemistry* :1-12(2013).  
<https://doi.org/10.1002/9780470027318.a9177>
- [37] [Talopin](#) D V and [Shevchenko](#) E V Introduction: Nanoparticle chemistry. *Chem. Rev.* **116**, 10343–10345(2016).  
<https://doi.org/10.1021/acs.chemrev.6b00566>
- [38] Michael T, Postek J The challenge of nanometrology. *Proc. SPIE* **4608**, 84–96, Nanostructure Science, Metrology, and Technology(2002).  
<https://doi.org/10.1117/12.427107>
- [39] Grégory G, Sergio M R, Francis L D. Nanomaterial properties: size and shape dependencies. *J of Nanomaterials* **180976**, 1-2(2012).  
<https://doi.org/10.1155/2012/180976>
- [40] Martínez L et al. Precisely controlled fabrication, manipulation and in-situ analysis of Cu based nanoparticles. *Scientific Reports* **8**, 7250, 1:3(2018).  
<https://doi.org/10.1038/s41598-018-25472-y>
- [41] [Donald R B](#), [Mark H E](#), Grant E J, Julia L, Jinfeng L, Karl M et al. Surface characterization of nanomaterials and nanoparticles: Important needs and challenging opportunities. *J Vac Sci Technol A* **31**, 050820(2013). <https://doi.org/10.1116/1.4818423>
- [42] [Donald Baer](#) R et al. Surface characterization of nanomaterials and nanoparticles: Important needs and challenging opportunities. *J Vac Sci Technol A*, **31**, 1–34(2013). <https://doi.org/10.1116/1.4818423>
- [43] Stefanos M, Roger M P, Nguyen T K T. Characterization techniques for nanoparticles: comparison and complementarity upon studying nanoparticle properties. *Nanoscale* **10**, 12871–12934(2018). <https://doi.org/10.1039/C8NR02278J>
- [44] [Carney](#) R et al. Determination of nanoparticle size distribution together with density or molecular weight by 2D analytical ultracentrifugation. *Nature Communications* **2**(1), 335(2011). <https://doi.org/10.1038/ncomms1338>
- [45] Sheglov D V et al. High-precision nanoscale length measurement. *Nanotechnologies in Russia* **8**, 518–531(2013). <https://doi.org/10.1134/S1995078013040162>
- [46] Mourdikoudis S, Pallares R M and Thanh N T K. Characterization techniques for nanoparticles: comparison and complementarity upon studying nanoparticle properties. *Nanoscale* **10**, 12871–12934.(2018). <https://doi.org/10.1039/C8NR02278J>
- [47] Sayed R, Saad H, Hagagy N. Silvernanoparticles: characterization and antibacterial properties. *Rendiconti Lincei Scienze Fisiche e Naturali* **29**, 81–86(2018). <https://doi.org/10.1007/s12210-017-0663-6>
- [48] Kovarik T et al. Particle size analysis and characterization of nanodiamond dispersions in water and dimethylformamide by various scattering and diffraction methods. *J Nanopart Res* **22**; 1-17(2020).  
<https://doi.org/10.1007/s11051-020-4755-3>



- [49] Ibrahim K, Khalid S and Idrees K. Nanoparticles: Properties, applications and toxicities. *Arabian Journal of chemistry* **12**, 908-931(2017). <https://doi.org/10.1016/j.arabjc.2017.05.011>
- [50] Mahmoudi M. The need for robust characterization of nanomaterials for nanomedicine applications. *Nature Communications* **12**(5246), 1-5(2021). <https://doi.org/10.1038/s41467-021-25584-6>
- [51] Pei-Jia Lu et al. Methodology for sample preparation and size measurement of commercial ZnO nanoparticles. *J of food and drug analysis* **26**, 628-636(2018). <https://doi.org/10.1016/j.jfda.2017.07.004>
- [52] Bell S. A Beginner's guide to uncertainty of measurement. *Measurement Good Practice Guide No.* **11**, 11-12(2001).
- [53] Kirkup L, Frenkel R B. An introduction to uncertainty in measurement. Cambridge University Press(2007). <https://doi.org/10.1017/CBO9780511755538>
- [54] Chicea D. Assessing Fe<sub>3</sub>O<sub>4</sub> nanoparticle size by DLS, XRD and AFM. *J of Optoelectronics and advanced materials* **14**, 460 – 466(2012).
- [55] Pabisch S et al. Effect of interparticle interactions on size determination of zirconia and Silica based systems – A comparison of SAXS, DLS, BET, XRD and TEM. *Chemical Physics Letters* **521**, 91-97(2012). <https://doi.org/10.1016/j.cplett.2011.11.049>
- [56] Sagadevan S and Koteeswari P. Analysis of structure, surface morphology, optical and electrical properties of copper nanoparticles. *J of Nanomedicine Research* **2**, 133-136(2015). <https://doi: 10.15406/jnmr.2015.02.00040>
- [57] Sayed R. and Saad H. Gold nanoparticles: green synthesis, characterization and biological activities. *Egy. J. Chem.* **64**, 7213-7222(2021). <https://doi: 10.21608/EJCHEM.2021.68846.3553>
- [58] Lawandy S N, Sayed R, Saleh B K, Halim S F. Utilization of nano-BS sand as filler in styrene butadiene rubber composites. *Egypt J Chem* **63**, 2051-2062(2020).
- [59] Jensen H, Pedersen J H et al. Determination of size distributions in nanosized powders by TEM, XRD, and SAXS. *J of Experimental Nanoscience* **1**, 355-373(2006). <https://doi.org/10.1080/17458080600752482>
- [60] Sharmal R, Bisen D P et al. X-ray diffraction: a powerful method of characterizing nanomaterials. *Recent Research in Science and Technology* **4**, 77-79(2012).
- [61] El-Akaad S, Mohamed M et al. 3D Bismuth ferrite microflowers electrochemical sensor for the multiple detection of pesticides. *J Electrochem Soc* **167**, 027543(2020). <https://doi:10.1149/1945-7111/ab6cf0>
- A practical approach. *Iranian J of Materials Science & Engineering* **8**, 48-56(2011).
- [73] Giannini C, Ladisa M et al. X-ray diffraction: a powerful technique for the multiple-length-scale
- [62] Sathiya C K and Akilandeswari S. Fabrication and characterization of Silvernanoparticles using Delonix elata leaf broth. *Acta Part A: Mol Biomol Spectrosc* **128**, 337-341(2014). <https://doi.org/ 10.1016/j.saa.2014.02.172>
- [63] Selvi BCG, Madhavan j and Santhanam A. Cytotoxic effect of Silvernanoparticles synthesized from Padina tetrastratica on breast cancer cell line. *Adv Nat Sci: Nanosci Nanotechnol* **7**, 1-8(2016). <https://doi:10.1088/2043-6262/7/3/035015>
- [64] Bin Ahmad M, Shameli K, Darroudi M et al. Synthesis and characterization of silver/clay nanocomposites by chemical reduction method. *American J of Applied Sciences* **6**, 1909-1914(2009).
- [65] Majid D, Mansor A, Abdul Halim A, Azowa N. Green synthesis and characterization of gelatin-based and sugar-reduced Silvernanoparticles. *Int J Nanomed* **6**, 569–574(2011). <https://doi: 10.2147/IJN.S16867>
- [66] Kamyar S, Mansor A, Seyed D J, Parvaneh S, Hossein J, Yadollah G. Investigation of antibacterial properties Silvernanoparticles prepared via green method. *Chem Central J* **6**, 1-10(2012). <http://journal.chemistrycentral.com/content/6/1/73>
- [67] Phanjom P and Ahmed G. Biosynthesis of Silvernanoparticles by aspergillus oryzae (MTCC No. 1846) and its characterizations. *Nanoscience and Nanotechnology* **5**, 14-21(2015). <https://doi: 10.5923/j.nn.20150501.03>
- [68] Vasudeva R N, Suman B, Latha D, Soneya S, Sindhu G, Murali S, Venkata S, Saritha K, Vijaya T. Biogenesis of Silvernanoparticles using leaf extract of Indigofera hirsuta L. and their potential biomedical applications (3-in-1 system). *Artif Cells Nanomed Biotechnol* **46**, 1138-1148(2018). <https://doi.org/ 10.1080/21691401.2018.1446967>
- [69] Liangwei D U, Liang X and Jia-Xun F. Rapid extra-/intracellular biosynthesis of Gold nanoparticles by the fungus Penicillium sp. *J. Nanopart Res* **13**, 921–930(2011). <https://doi 10.1007/s11051-010-0165-2>
- [70] S W Shivaji, M D Arvind, S Zygmunt (2014) Biosynthesis, optimization, purification and characterization of Gold nanoparticles. *Afr J Microbiol Res* **8**, 138-146. <https://doi:10.5897/AJMR10.143>
- [71] Senthilkumar S, Kashinath L, Ashok M and Rajendran A. Antibacterial properties and mechanism of Gold nanoparticles obtained from pergularia daemia leaf extract. *J of Nanomed Res* **6**, 1-5(2017). <https://doi: 10.15406/jnmr.2017.06.00146>
- [72] Akbari B, Pirhadi Tavandashti M and Zandrahimi M. Particle size characterization of nanoparticles structural analysis of nanomaterials. *Crystals* **6**, 1-22(2016). <https://doi:10.3390/cryst6080087>